

Compact Models for Asymmetric Double Gate MOSFETs

Hedley Morris*, Henok Abebe**, Ellis Cumberbatch***

*Department of Mathematics, San Jose State University

San Jose, CA 95192, USA, FAX: (408) 924-5080, morris@math.sjsu.edu

**University of Southern California, Information Sciences Institute, MOSIS service

Marina del Rey, CA 90292, USA. Tel: (310) 448-8740,

Fax: (310) 823-5624, e-mail: abebeh@mosis.org

***Claremont Graduate University, School of Mathematical Sciences

710 N College Ave, Claremont, CA 91711, USA. Tel: (909) 607-3369,

Fax: (909) 621-8390, e-mail: ellis.cumberbatch@cgu.edu

ABSTRACT

Double-gate MOSFET's are one possible option to further extend CMOS scaling when planar MOSFET's have reached their scaling limit. This paper presents an analytic potential model for long-channel asymmetric double-gate (ADG) MOSFETs. The asymmetry is due to a difference in the work functions of the two gates. Taur has derived equations from the exact solution to Poisson's and current continuity equation without the charge-sheet approximation. In previous work by the authors it was shown that, by means of the Lambert function, compact formulae could be derived from Taur's equations for the symmetric double-gate (SDG) case. In this paper we show that these results of can be extended to the asymmetric case and we construct generalized compact formulae for an ADG device that are suitable for use in SPICE type simulators.

Keywords: Analytic solutions, compact model, double gate MOSFETs.

1 INTRODUCTION

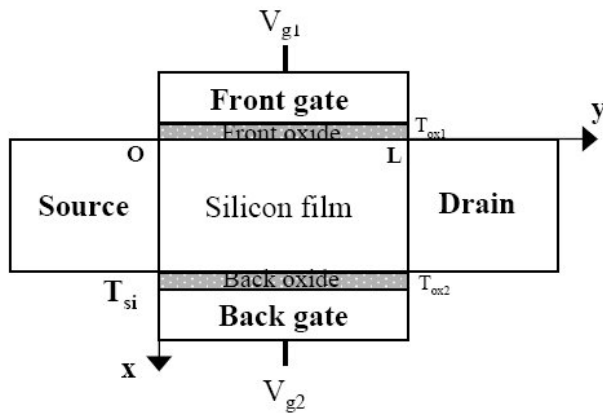


Figure 1. The structure of an asymmetric double gate MOSFET

| T_{si} | T_{ox} | $\Delta\phi_1$ | $\Delta\phi_2$ |
|----------|----------|----------------|----------------|
| 10nm | 1.5nm | -0.56 | 0.56 |

Table 1. Device constants

A Compact models for double gate (DG) MOSFETs is of interest, due to the potential of these design geometries as replacements for the standard planar MOSFET in the nanometer regime. In this paper we assume the two oxide thicknesses are the same, $T_{ox1} = T_{ox2} = T_{ox}$ and the device parameters are those given in Table 1. In [1-5] Taur et al. have developed a series of models for an undoped double-gate device. The absence of doping in the silicon channel allows explicit integration of the Poisson equation in the quasi-1-D approximation. The Poisson equation in the quasi-1-D approximation reads:

$$\frac{d^2\psi}{dx^2} = \frac{q}{\epsilon_{si}} n_i e^{q(\psi-V)/kT} \quad (1)$$

where q is the electric charge, ϵ_{si} is the permittivity of silicon, n_i is the intrinsic carrier density, $\psi(x)$ is the electrostatic potential and V is the electron quasi-fermi potential. The hole density is regarded as negligible. For the ADG the boundary conditions at the two oxide surfaces are given by

$$\epsilon_{ox} \frac{V_g - \Delta\phi_1 - \psi_{s1}}{T_{ox}} = -\epsilon_{si} \frac{d\psi}{dx} \Big|_{x=-\frac{T_i}{2}} \quad (2)$$

$$\epsilon_{ox} \frac{V_g - \Delta\phi_2 - \psi_{s2}}{T_{ox}} = \epsilon_{si} \frac{d\psi}{dx} \Big|_{x=\frac{T_i}{2}} \quad (3)$$

where ψ_{s1} and ψ_{s2} are surface potentials. A solution to the Poisson equation (1) is given by

$$\psi(x) = V - 2 \frac{kT}{q} \ln \left(\frac{T_{si}}{2\beta} \sqrt{\frac{q^2 n_i}{2\epsilon_{si} kT}} \sin \left(\frac{2\beta x}{T_{si}} + \alpha \right) \right) \quad (4)$$

involving parameters α and β to be determined by the boundary conditions obtained by substituting (4) into (2-3)

$$V_g - V = c_1 + 2 \frac{q}{kT} \ln \frac{2\beta}{\sin(\alpha - \beta)} + 4 \frac{q}{kT} r\beta \cot(\alpha - \beta) \quad (5)$$

$$V_g - V = c_2 + 2V_{th} \ln \frac{2\beta}{\sin(\alpha + \beta)} - 4V_{th} r\beta \cot(\alpha + \beta) \quad (6)$$

where $c_{1,2} = V_{th} \ln\left(\frac{2\varepsilon_{si} V_{th}}{qn_i T_{si}^2}\right) + \Delta\phi_{1,2}$ and $\Delta\phi_{1,2}$ are the

work function differences between the two gates and

intrinsic silicon and $r = \frac{\varepsilon_{si} T_{ox}}{\varepsilon_{ox} T_{si}}$. Subtracting (6) from (5)

yields the equivalent equations

$$\ln \frac{\sin(\alpha + \beta)}{\sin(\alpha - \beta)} + 2r\beta(\cot(\alpha - \beta) + \cot(\alpha + \beta)) - \delta = 0 \quad (7)$$

$$V_g - V = c_1 + 2 \frac{q}{kT} \ln \frac{2\beta}{\sin(\alpha - \beta)} + 4 \frac{q}{kT} r\beta \cot(\alpha - \beta) \quad (8)$$

where $\delta = \frac{q}{2kT}(\Delta\phi_2 - \Delta\phi_1)$. Equation (7) together with

(5) can be solved numerically to obtain α and β as

functions of $V_g - V$. In [1] Taur shows that the total

inversion charge Q_i is given by

$$Q_i = \frac{4\varepsilon_{si}}{T_{si}} \frac{kT}{q} \beta(\cot(\alpha - \beta) - \cot(\alpha + \beta)) \quad (9)$$

As explained in detail in Taur [1] the solution (4) is only valid for $V - V_g$ above a critical value V_{crit} . Below that

critical voltage level the solution (4) is replaced by the alternative hyperbolic solution

$$\psi(x) = V - 2 \frac{kT}{q} \ln\left(\frac{T_{si}}{2\bar{\beta}} \sqrt{\frac{q^2 n_i}{2\varepsilon_{si} kT}} \sinh\left(\frac{2\bar{\beta}x}{T_{si}} + \bar{\alpha}\right)\right)$$

and (7-9) are replaced by

$$\ln \frac{\sinh(\bar{\alpha} + \bar{\beta})}{\sinh(\bar{\alpha} - \bar{\beta})} + 2r\bar{\beta}(\coth(\bar{\alpha} - \bar{\beta}) + \coth(\bar{\alpha} + \bar{\beta})) - \delta = 0$$

$$V_g - V = c_1 + 2 \frac{q}{kT} \ln \frac{2\bar{\beta}}{\sinh(\bar{\alpha} - \bar{\beta})} + 4 \frac{q}{kT} r\bar{\beta} \cot(\bar{\alpha} - \bar{\beta})$$

$$Q_i = \frac{4\varepsilon_{si}}{T_{si}} \frac{kT}{q} \bar{\beta}(\cot(\bar{\alpha} - \bar{\beta}) - \cot(\bar{\alpha} + \bar{\beta}))$$

In the next section we will construct analytic solutions to (7-8) and (10).

2 ANALYTIC SOLUTIONS

In previous work [6-7] we have developed analytic formulae for Symmetric Double Gate (SDG) devices with various geometries. In this paper we construct analytic solutions to equations (5) and (7). To do so we introduce

the new variable θ defined by $\theta = \frac{2\beta}{\sin(\alpha - \beta)}$ which can

be solved to give

$$\alpha = \beta + \sin^{-1}\left(\frac{2\beta}{\theta}\right) \quad (10)$$

If we use (10) in (7) and approximate $\cos(\alpha - \beta)$ by unity, then (7) reduces to the simple form

$$\ln(\theta) + r\theta = U \quad (11)$$

where $U = \frac{q}{2kT}(V_g - V - c_1)$. Equation (11) has the

solution

$$\theta = \frac{1}{r} \text{LambertW}(re^U) \quad (12)$$

The solution is given in terms of the Lambert function [8]

for which there are fast algorithms. A similar technique

was used for the SDG and details can be found in [6-7].

Using (10) in (8) and approximating $\cos(\alpha - \beta)$ by unity,

yields the transcendental equation

$$\delta - U = \ln\left(\frac{\sin(2\beta)}{2\beta}\right) + 2r\beta \cot(2\beta) \quad (13)$$

for β . This equation is easily solved for β by a Newton

scheme. Thus (11) and (13) provide a fast algorithm for

determining α and β as functions of the voltage V .

Figure 1 shows a comparison of the numerical and analytic solution for β as a function of α .

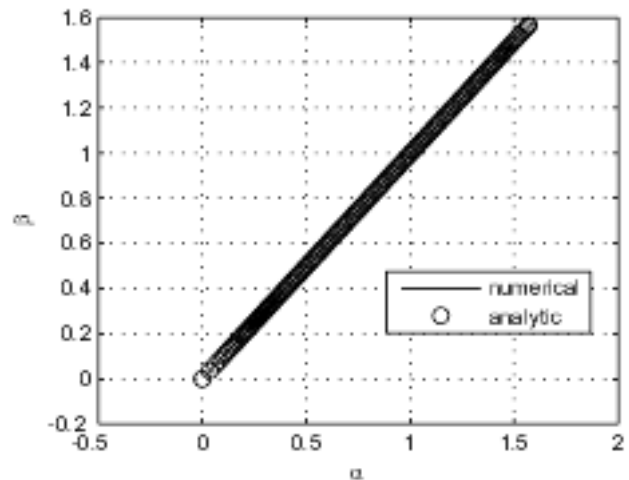


Figure 1. A plot of β versus α .

The range of α has been restricted to $(0, \frac{\pi}{2})$ as the (α, β) solution (4) joins to the hyperbolic solution $(\bar{\alpha}, \bar{\beta})$ at $(0, 0)$.

3 THE HYPERBOLIC SOLUTION

The hyperbolic solution involving $(\bar{\alpha}, \bar{\beta})$ can be treated in a very similar manner to the (α, β) . We only consider negative values of $\bar{\alpha}$ and $\bar{\beta}$ as this is the range that matches to the solution of the previous section at $(0, 0)$. Equations (10) and (13) are replaced by their hyperbolic counterparts

$$\bar{\alpha} = \bar{\beta} + \sinh^{-1}\left(\frac{2\bar{\beta}}{\theta}\right) \quad (14)$$

$$\delta - U = \ln\left(\frac{\sinh(2\bar{\beta})}{2\bar{\beta}}\right) + 2r\bar{\beta} \coth(2\bar{\beta}) \quad (15)$$

The variables U, θ remain as defined previously. Figure 2 shows the hyperbolic solutions for a range of negative value of $\bar{\alpha}$ and $\bar{\beta}$.

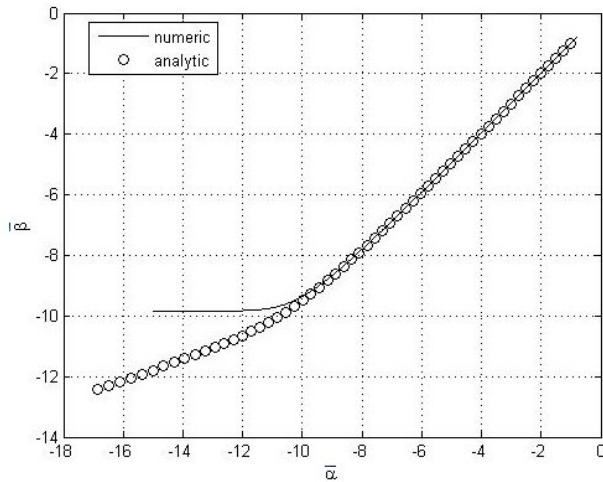


Figure 2. A plot of $\bar{\beta}$ versus $\bar{\alpha}$.

The value of $\bar{\beta}$ saturates at a value $\bar{\beta}_\infty \sim -\frac{\delta}{2+4r}$. Clearly our approximate solution fails for $\bar{\beta} \sim -10$ but this is of no consequence as the intrinsic charge is negligible for such values.

4 JOINING THE SOLUTIONS

The two solutions must match as both (α, β) and $(\bar{\alpha}, \bar{\beta})$ approach $(0, 0)$ with $\alpha/\beta = \bar{\alpha}/\bar{\beta} = s$. This will also an exact formula for the critical voltage as a function of device parameters. The common slope value $s = \alpha/\beta = \bar{\alpha}/\bar{\beta}$ must satisfy the equation

$$\ln \frac{s+1}{s-1} + r\left(\frac{s+1}{s-1} - \frac{s-1}{s+1}\right) - \delta = 0 \quad (16)$$

If we introduce $s = \coth(\frac{\xi}{2})$ equation (16) can be written

$$\xi + 2r \cosh(\xi) - \delta = 0 \quad (17)$$

If $\delta > 0$ and $e^\xi \ll 1$ we can assume $\cosh(\xi) \sim \frac{1}{2}e^\xi$ and

an analytic solution for ξ is given by

$$\xi = \delta - \text{LambertW}(re^\xi) \quad (18)$$

Once s has been found the critical voltage is given from

$$V_{crit} = c_1 + \frac{2kT}{q} \left(\ln\left(\frac{2}{s-1}\right) + \frac{2r}{q} \frac{1}{s-1} \right) \quad (19)$$

$\Delta\phi_1 = -0.56, \Delta\phi_2 = 0.56$

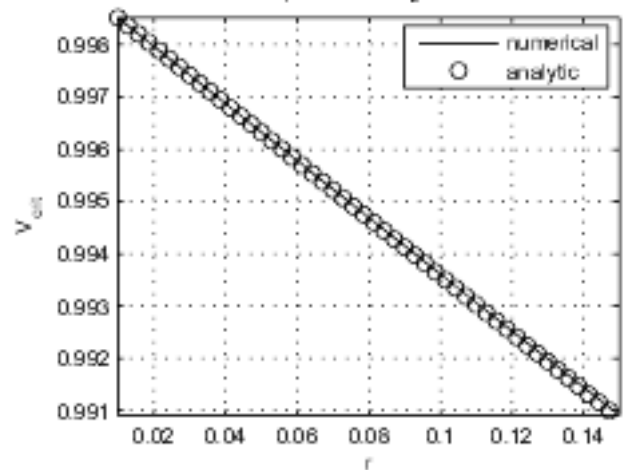


Figure 3. The variation of V_{crit} with the device parameter r .

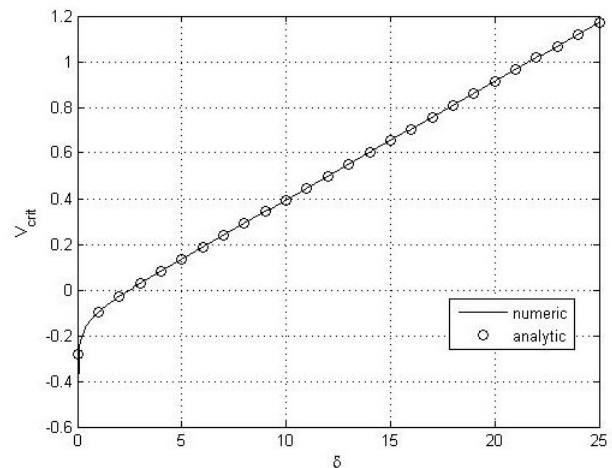


Figure 4. The variation of V_{crit} with the δ .

The dependence on the work function difference can be seen from Figure 4.

5 THE INTRINSIC CHARGE

From α and β we can obtain the charge using (9).

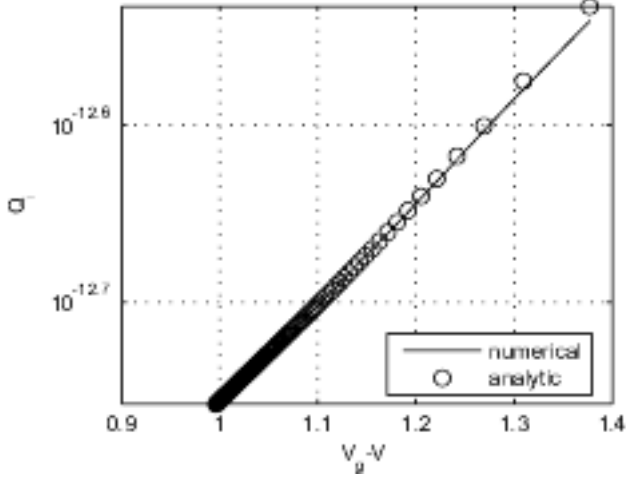


Figure 5. A plot of Q versus $V_g - V$.

Figure 5 shows the true Q_i calculated numerically in comparison with that obtained using the analytic formulae.

6 DEVICE CHARACTERISTICS

From Q_i the current is obtained from the usual formula

$$I_{ds} = \mu \frac{W}{L} \int_{V_s}^{V_d} Q_i(V) dV \quad (20)$$

An analytic approximation for Q_i is given by

$$Q_i = \frac{4\epsilon_{si}}{T_{si}} \frac{kT}{q} \left(\frac{\theta}{2} - \beta \cot(2\beta) \right) \quad (21)$$

If we substitute (21) into (20) we can write

$$I_{ds} = \mu \frac{W}{L} \frac{4\epsilon_{si}}{T_{si}} \frac{kT}{q} (J_1 - J_2) \quad (22)$$

where

$$J_1 = \int_{\theta_s}^{\theta_d} \frac{1}{2} \theta \frac{dV}{d\theta} d\theta \quad (23)$$

and

$$J_2 = \int_{\beta_s}^{\beta_d} \beta \cot(2\beta) \frac{dV}{d\beta} d\beta \quad (24)$$

From (12) we obtain

$$\frac{dV}{d\theta} = -2 \frac{kT}{q} \left(r + \frac{1}{\theta} \right) \quad (25)$$

This allows J_1 to be easily evaluated as

$$J_1 = -\frac{kT}{q} \left[\frac{1}{2} r \theta^2 + \theta \right]_{\theta_s}^{\theta_d} \quad (26)$$

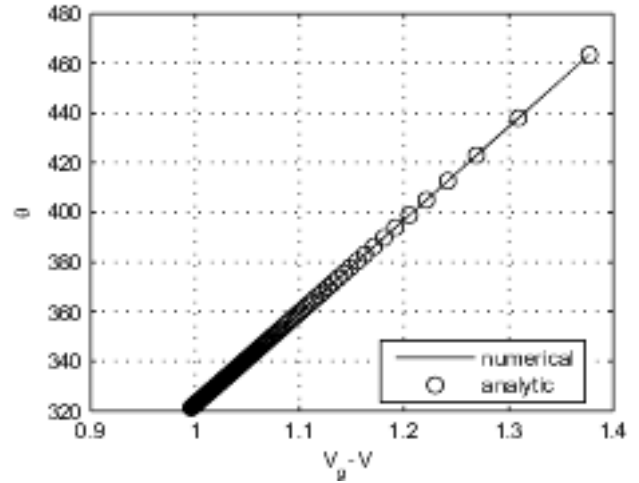


Figure 6. A plot of θ versus $V_g - V$.

To evaluate J_1 we obtain θ from $\theta = \frac{2\beta}{\sin(\alpha - \beta)}$ using our analytic forms for α and β . Figure 6 shows the variation of θ with $V_g - V$. From (13) we obtain

$$\frac{dV}{d\beta} = 2 \frac{kT}{q} (2 \cot(2\beta)(1+r) - \frac{1}{\beta} - 4r\beta \csc^2(2\beta)) \quad (27)$$

This allow to write J_2 in the exact form

$$J_2 = 2 \frac{kT}{q} (2(1+r)I_1 - I_2 - 4rI_3) \quad (28)$$

with

$$I_1 = \int_{\beta_s}^{\beta_d} \beta \cot^2(2\beta) d\beta = F_1(\beta_d) - F_1(\beta_s) \quad (29)$$

$$I_2 = \int_{\beta_s}^{\beta_d} \cot(2\beta) d\beta = F_2(\beta_d) - F_2(\beta_s) \quad (30)$$

$$I_3 = \int_{\beta_s}^{\beta_d} \beta \cot(2\beta) \csc^2(2\beta) d\beta = F_3(\beta_d) - F_3(\beta_s) \quad (31)$$

involving the explicit functions

$$F_1(\beta) = \frac{1}{8} \ln(\sin^2(2\beta)) - \frac{1}{2} \beta^2 - \frac{1}{2} \beta \cot(2\beta)$$

$$F_2(\beta) = \frac{1}{4} \ln(\sin^2(2\beta))$$

$$F_3(\beta) = -\frac{1}{4} \beta^2 \csc^2(2\beta) - \frac{1}{4} \beta \cot(2\beta) + \frac{1}{8} \ln(\sin(2\beta))$$

For the hyperbolic solution the intrinsic charge can be approximated by

$$Q_i = \frac{4\epsilon_{si}}{T_{si}} \frac{kT}{q} \left(\frac{\theta}{2} - \beta \coth(2\beta) \right) \quad (32)$$

By a similar process to the non-hyperbolic case, exact formulae for the currents can be obtained for the hyperbolic case also. Full results will be reported elsewhere.

7 CONCLUSION

We have shown that by using asymptotic methods accurate analytic formulae can be derived for the characteristics of an ADG device. These results allow Fast algorithms for use in SPICE type simulators.

REFERENCES

- [1] H. Lu and Y. Taur, "An Analytic Potential Model for Symmetric and Asymmetric DG MOSFETs," IEEE Trans. Electron Devices, Vol. 53, No. 5, May 2006.
- [2] H. Lu and Y. Taur, "Physics-Based, Non-Charge-Sheet Compact Modeling of Double Gate MOSFETs," Nanotech, Anaheim, Ca., 2005.
- [3] Y. Taur, X. Liang, W. Wang and H. Liu, "A continuous, analytic drain-current model for DG-MOSFETs," IEEE Electron Device Lett., vol 25., no.2, pp. 107-109, 2004.
- [4] Y. Taur, "An analytical Solution to a Double-Gate MOSFET with Undoped Body," IEEE Electron Device Lett , vol 21., no.5, pp. 245-247, 2000.
- [5] X. Liang, Y. Taur, "A 2-D Analytical Solution for SCEs in DG MOSFETs", IEEE Trans. Electron Devices, Vol. 51, No. 8, August 2004.
- [6] H. Morris, E. Cumberbatch, H. Abebe, S. Uno, "Compact Models for Double Gate and Surround Gate MOSFET's", Technical Proceedings of the 2006 NSTI Nanotechnology Conference, Vol 3 , May 2006, 824 - 827 (2006).
- [7] H. Morris, H. Abebe, E. Cumberbatch and V. Tyree, "Compact Models for the I-V Characteristics of Double Gate and Surround Gate MOSFETs", IEEE UGIM Proceedings, ISBN: 1-4244-0267-0, pp. 117-121, June 25-28, 2006, San Jose, CA. (2006)
- [8] R. Corless, G. Gonnet, D. Hare, D. Jeffrey, and D. Knuth, "On the Lambert W function", Advances in Computational Mathematics 5(4): 329-359 (1996).